Signaling Molecules in the Fetal Rabbit Model for Congenital Diaphragmatic Hernia

Aline Vuckovic, MD,[1]* Xenia I. Roubliova, MD, PhD,[2] Carmela Votino, MD, PhD,[3] Robert Naeije, MD, PhD,[1] and Jacques C. Jani, MD, PhD[3]

Summary. Rationale and objectives: Little is known about molecular changes in lungs of fetal rabbits with surgically induced diaphragmatic hernia (DH). Therefore, we examined in this model gene expressions of pivotal molecules for the developing lung. Methods: At day 23 of gestation, DH was created in 12 fetuses from 4 does. Both lungs from six live DH fetuses and from six unoperated controls were harvested and weighed at term. Transcription of 15 genes involved in alveolarization, angiogenesis, regulation of vascular tone, or epithelial maturation was investigated by real-time quantitative polymerase chain reaction. Main results: DH decreased lung-to-body weight ratio ($P < 0.001$). A bilateral downregulation was seen for genes encoding for tropoelastin ($P < 0.01$), lysyl oxidase ($P < 0.05$), fibulin 5 ($P < 0.05$), and cGMP specific phosphodiesterase 5 ($P < 0.05$). Lower mRNA levels for endothelial nitric oxide synthase occurred in the ipsilateral lung ($P < 0.05$). Conclusions: Experimental DH in fetal rabbits disrupted transcription of genes implicated in lung growth and function. Similarities with the human disease make this model appropriate for investigation of new prenatal therapies.
Pediatr Pulmonol. © 2012 Wiley Periodicals, Inc.

Key words: alveolarization; angiogenesis; lung development; gene expression; lung hypoplasia.

Funding source: Fonds de la Recherche Scientifique (FNRS).

INTRODUCTION

Despite advances in prenatal diagnosis and resuscitation, congenital diaphragmatic hernia (CDH) has a persistent high mortality rate due to ventilatory insufficiency and neonatal pulmonary hypertension.[1] CDH results in pulmonary hypoplasia with airway and vascular changes that are more predominant in the ipsilateral lung. Recent findings in human CDH lungs have enriched the understanding of the disease, pointing out preserved contents of pulmonary surfactant-associated proteins (SP),[2] impaired alveolarization with deficient tropoelastin (ELN),[3] and altered angiogenesis linked to a downregulation of endothelial nitric oxide synthase (eNOS), which could not be counteracted by vascular endothelial growth factor A (VEGFA).[4] Besides these rare human investigations, animal experimentation has helped to understand the pathogenesis of CDH and to optimize new therapies modulating lung growth, like tracheal occlusion (TO).[5] On the one hand, genetic and teratogenic models in rodents have contributed to the partial comprehension of mechanisms responsible for the early disturbed lung growth.[6] On the other hand, much of current knowledge about how TO proceeds originates from surgical studies in rabbits[7,8] and sheep.[9]

The creation of a diaphragmatic hernia (DH) in rabbit fetuses during the pseudoglandular phase of lung development recapitulates most histological[10,11] and functional features[12] of human CDH lungs. However, very little if any emphasis has been placed on biological changes occurring in the rabbit model. Therefore, we used real-time quantitative polymerase chain reaction (qPCR) to study in this model pulmonary expression of specific genes involved in alveolarization, angiogenesis,

[1]Laboratory of Physiology and Physiopathology, Faculty of Medicine, Université Libre de Bruxelles, Brussels, Belgium.

[2]HistoGeneX, Antwerpen, Belgium.

[3]Department of Obstetrics and Gynecology, University Hospital Brugmann, Brussels, Belgium.

Conflict of interest: None.

*Correspondence to: Aline Vuckovic, MD, Laboratory of Physiology and Physiopathology, Faculty of Medicine, Université Libre de Bruxelles, Route de Lennik 808, B-1070 Bruxelles, Belgium.
E-mail: avuckovi@ulb.ac.be

Received 12 August 2011; Accepted 5 January 2012.

DOI 10.1002/ppul.22512
Published online in Wiley Online Library (wileyonlinelibrary.com).

regulation of vascular tone, or epithelial cell maturation. The objectives were to determine whether the rabbit model reproduced biological aspects of human CDH, and to study other crucial molecules for late pulmonary development, which have never been examined in the setting of human CDH.

MATERIALS AND METHODS

Animal Subjects

Four time-dated pregnant New Zealand white rabbits were obtained at 15 days' gestational age (GA) from an authorized farm. Animals were housed separately at normal room temperature in a regular light–dark cycle, with free access to pellets, hay, and water. The experiments were carried out according to the current guidelines on animal wellbeing, and approved by the local Ethics Committee for Animal Experimentation (Faculty of Medicine, Université Libre de Bruxelles, Brussels, Belgium).

Premedication, Anesthesia, and Surgery

At 23 days' GA, each rabbit was premedicated as previously reported.[12] After fiberoptic endotracheal intubation,[13] mechanical ventilation was initiated under general anesthesia with 1–2% isoflurane. Heart rate and oxygen saturation were monitored with a pulse oximeter. Body temperature was maintained with a heating pad. Just prior to surgery, prophylactic antibiotics and progesterone for tocolysis were administered. Briefly, three fetuses per doe were subjected to an incision of the membranous part of the diaphragm through a left thoracotomy.[10–12] After surgery, the does were monitored until awakening. They were then returned to their cages with free access to food and water.

Fetal Tissue Collection

At term (31 days' GA), fetuses were exposed by a cesarean section. Live operated fetuses were recorded. Unoperated littermates of equal size to the operated ones were taken as controls. Before clamping the umbilical chord, neonatal rabbits received a ketamine–xylazine mixture to avoid respiratory movements. After recording body weight, the chest was opened and pups were killed by exsanguination. Lungs were dissected, weighed separately to assess the wet lung to body weight ratio (LBWR), snap-frozen in liquid nitrogen, and stored at −80°C. Maternal anesthesia was maintained during fetal harvesting. As soon as all fetuses were delivered, the doe was killed with an overdose of sodium pentobarbital.

RNA Extraction and Quality

Total RNA was isolated from left and right frozen lung samples using TRIzol reagent (Invitrogen, Ghent, Belgium), and purified with spin columns according to the manufacturer's protocol (RNeasy Mini Kit, Qiagen, Venlo, The Netherlands). RNA concentrations were quantified at 260 nm (NanoDrop 2000, Thermoscientific, Wilmington, DE). RNA integrity was confirmed by 1.5% agarose gel electrophoresis. The absence of genomic DNA was verified by qPCR performed on isolated RNA.

Reverse Transcription

For each sample, first strand cDNA synthesis was performed in duplicate with 2 μg of total RNA in a 20-μl total reaction volume containing random hexamers, a mix of deoxyribonucleotides, reverse transcription buffer, dithiothreitol, ribonuclease inhibitor, and Superscript II reverse transcriptase following the manufacturer's instructions (Invitrogen). The reaction was conducted in a thermal cycler (Mastercycler, Eppendorf AG, Hamburg, Germany), using the following conditions: 25°C for 10 min, 42°C for 50 min, and 70°C for 15 min.

Primer Design and Validation

Primer pairs for target and reference genes were generated by the program Primer3 (http://frodo.wi.mit.edu/primer3/) using rabbit or human nucleic acid sequences from GenBank (Tables 1 and 2). The absence of secondary structures in the region in which the primers anneal was verified using Mfold program (http://mfold.rna.albany.edu/). A BLAST analysis was run to check if primer pairs were matching at the sequence of interest (http://www.ncbi.nlm.nih.gov/BLAST/). Newly designed primers were synthesized at Eurogentec (Liège, Belgium). PCR efficiencies in the exponential phase were calculated by standard curves run in triplicate, according to the equation $E = 10^{[-1/\text{slope}]}$, and were all between 1.93 and 2.14. The generation of a single specific product was confirmed by melting curve analysis, and documented with 2.5% agarose gel electrophoresis (Fig. 1).

Real-Time Quantitative Polymerase Chain Reaction (qPCR)

SYBR Green qPCR analysis was carried out with the Icycler iQ detection system (Bio-Rad Laboratories, Hemel Hempstead, UK). For each gene, the procedure was realized in triplicate with a 25-μl reaction volume containing 12.5 ng of cDNA, 5 pmol/μl of each primer, and 12.5 μl of SYBR Green PCR Master Mix (Quanta Biosciences, Gaithersburg, MD). Amplification was conducted as follows: initial denaturation (95°C for 3 min), amplification program repeated 40 times (15 sec at 95°C followed by 1 min at 60°C), and melting curve program (starting temperature of 95°C and ending temperature of 60°C at 0.5°C increments). To ensure the quality of

TABLE 1— Characteristics of Primers Used for qPCR Analysis of Target Genes

Gene symbol (GenBank accession)	Primer Sequences	T_m (°C)
DBN1 (NM001082149)	F: 5′-GGAAATGAAACGCATCAACC-3′	60.32
	R: 5′-CTTCTTCCGCTCCTCTTCCT-3′	60.09
	Amplicon size: 85 bp	
ELN (XM002721971)	F: 5′-AGCCAAATACGGTGCTGCT-3′	60.81
	R: 5′-CACCTGGGTAAATGGGAGAC-3′	59.26
	Amplicon size: 110 bp	
eNOS (NM001082733)	F: 5′-ACAGTTACCAGCTCGCCAAA-3′	60.83
	R: 5′-GCTCATTCTCCAGGTGCTTC-3′	59.96
	Amplicon size: 81 bp	
FBLN5 (XM002719596)	F: 5′-CAACTACCCCACGATTTCCA-3′	60.74
	R: 5′-TCCACATCCACACACTGGTT-3′	59.85
	Amplicon size: 81 bp	
LOX (XM002710146)	F: 5′-CCCCCAACGAGTGAAAAAC-3′	60.34
	R: 5′-ATGCTGTGGTAATGCTGGTG-3′	59.6
	Amplicon size: 99 bp	
PDE5 (NM001083)	F: 5′-AAAAGCCACCAGAGAAATGG-3′	59.17
	R: 5′-GCAAGGGACAAGAGCAAGAT-3′	59.43
	Amplicon size: 110 bp	
sGCα1 (XM002716887)	F: 5′-CTAAAGAAGAGGCTGGGGAAG-3′	60.15
	R: 5′-CGCAGGGAAAGATAGAGCA-3′	59.37
	Amplicon size: 109 bp	
sGCß1 (XM002716886)	F: 5′-TGTCCGTCTTCTCTCTGGTTC-3′	59.44
	R: 5′-TCCAACAATCCTTCCTTGCT-3′	59.67
	Amplicon size: 106 bp	
SPA (NM001082229)	F: 5′-ACACAGATGGGAAGTGGAATG-3′	59.84
	R: 5′-AGGGAGGTGGAAAAGCAAG-3′	59.27
	Amplicon size: 120 bp	
SPB (NM001082343)	F: 5′-TCTACAGGAAGTCTGGGGACA-3′	59.71
	R: 5′-CCTTGGTCATCTTGGTTAGGA-3′	59.04
	Amplicon size: 89 bp	
SPC (NM001082322)	F: 5′-CATTGTCACCTGCGACTACC-3′	59.17
	R: 5′-TGCTGTCTGGAGCCATCTT-3′	59.52
	Amplicon size: 95 bp	
TNC (XM002720513)	F: 5′-TGAACTCTCCTACGGCATCA-3′	59.39
	R : 5′-TCATACTCGGTGTCAGGCTTC-3′	60.27
	Amplicon size: 111 bp	
VEGFA (XM002714697)	R: 5′-CTTGCCTTGCTGCTCTACCT-3′	59.78
	F: 5′-TCGTGGGGTTTATTGTCTCC-3′	59.79
	Amplicon size: 83 bp	
VEGFR1 (XM002721430)	R: 5′-CCCCGATTATGTGAGAAAAGG-3′	60.67
	F: 5′-TCGCTCTTGGTGCTGTAGATT-3′	60.03
	Amplicon size: 93 bp	
VEGFR2 (NM001195670)	R: 5′-CCGGCCTGTGAGTGTAAAA-3′	59.7
	F: 5′-GACTGGTTGTCATCTGGGACT-3′	59.02
	Amplicon size: 81 bp	

q-PCR, real time quantitative polymerase chain reaction; T_m, optimal hybridization temperature; F, forward primer; R, reverse primer; bp, base pairs.

measurements, we included negative (no template control) and positive controls in triplicate in each plate. At the end of each run, the Icycler software established a horizontal threshold through the exponential phase of the amplification plot where amplified DNA just became detectable above the background fluorescence. The fractional cycle at which this horizontal threshold crossed the exponential phase determined the cycle threshold (C_t), which was calculated for each well.

Identification of Optimal Reference Genes for Normalization of Target Gene Expression

No previous study has validated reference genes in the fetal rabbit lung (normal or diseased). We therefore assessed the expression stability of 10 candidate reference genes belonging to various functional classes and usually considered to be stable (Table 2).[14] For each candidate, qPCR was performed in triplicate in 12

TABLE 2— Characteristics of Primers Used for qPCR Analysis of Reference Genes and Ranking According to Their Expression Stability

Gene (GenBank accession #)	Primer sequences	T_m (°C)	M value
ACTB (NM001101683)	F: 5′-GATCTGGCACCACACCTTCT-3′	60.12	0.132
	R: 5′-TGATCTGGGTCATCTTCTCG-3′	58.75	
	Amplicon size: 116 bp		
ATP5B (XM002711084)	F: 5′-GAGGTCCCATCAAAACCAAA-3′	59.77	0.125
	R: 5′-TTTCCTGCTCCACACTCATCT-3′	59.86	
	Amplicon size: 81 bp		
B2M (XM002717921)	F: 5′-CGCCCCAGATTGATATTGAG-3′	60.43	0.22
	R: 5′-GGACCAGGAGATAGAAAGACCA-3′	59.58	
	Amplicon size: 105 bp		
GAPDH (NM001082253)	F: 5′-AGGTCGGAGTGAACGGATT-3′	59.52	0.235
	R: 5′-ATGGCGACAACATCCACTTT-3′	60.38	
	Amplicon size: 85 bp		
HMBS (XM002722723)	F: 5′-GGCAACGCTGAAAACCTTAT-3′	59.23	0.332
	R: 5′-AGGCTCTTCTCCCCAATCTT-3′	59.28	
	Amplicon size: 111 bp		
HPRT (NM001105671)	F: 5′-GGCAAAACAATGCAGACCTT-3′	60.12	0.204
	R: 5′-CTTCGAGGGGTCCTTTTCAC-3′	60.99	
	Amplicon size: 95 bp		
PGK1 (XM002709000)	F: 5′-CTAGGCGGAGCTAAAGTTGC-3′	59.27	0.256
	R: 5′-AGCCATTCCACCACCAATAA-3′	60.19	
	Amplicon size: 90 bp		
RPLP0 (XM002719794)	F:5′-ACCTCCTTTTTCCAGGCTTT-3′	59.21	0.179
	R: 5′-GCTCCCACTTTGTCTCCAGT-3′	59.3	
	Amplicon size: 104 bp		
SDHA (XM002723194)	F: 5′-ATCTATCAGCGTGCGTTCG-3′	59.99	0.158
	R: 5′-ATCAGCCACACAGCAGCAT-3′	60.45	
	Amplicon size: 81 bp		
TOP1 (NM001101683)	F: 5′-GCAGGCAATGAGAAGGAAGA-3′	60.48	0.118
	R: 5′-CACGTACTCCTGACCATCCA-3′	59.55	
	Amplicon size: 108 bp		

q-PCR, real time quantitative polymerase chain reaction; T_m, optimal hybridization temperature; F, forward primer; R, reverse primer; bp, base pairs.
The M value is a parameter of reference gene stability obtained from the geNorm algorithm. The lowest M value indicates the highest gene stability.

representative fetal lung samples, with or without DH. Raw C_t values were analyzed with the geNorm program (http://www.biogazelle.com/). This algorithm ranks reference genes based on the calculation of a stability parameter (M), which is the mean pair-wise variation for a gene from all other candidate reference genes.[14] All genes were stably expressed ($M < 0.5$; Table 2), with type 1 topoisomerase (TOP1), ATP synthase subunit ß (ATP5B), and ß-actin (ACTB) being the most stable genes. A combination of these three reference genes was therefore considered for normalization of target gene expressions.

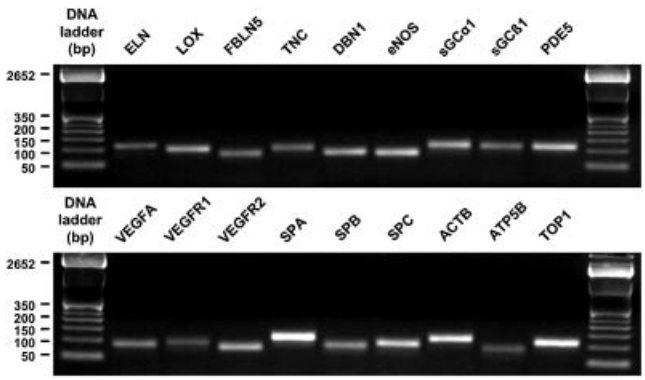

Fig. 1. Agarose gel electrophoresis of qPCR reaction products illustrating the specificity of primers used for gene expression analyses. bp = base pairs.

Analysis of qPCR Data

The mean C_t value was calculated in each sample for genes of interest and validated reference genes. Gene expression of an unknown sample was obtained relative to the sample with the lowest C_t value (ΔC_t) according to the efficiency corrected model.[15] For each target gene in each sample, expression levels were then normalized by the geometric mean of reference genes TOP1, ATP5B, and ACTB.[14] Relative expression levels of the target genes in DH lungs were expressed as a fold of increase, compared with expression level in

control lungs, which was as 1. Intra-assay and inter-assay coefficients of variation of C_t were below 1.2% and 1.1%, respectively.

Statistical Analysis

Data were reported as mean ± SEM. Body weights and LBWR were compared using an unpaired Student's *t*-test after ensuring normality and equality of variance. The differences in gene expressions between DH and control fetuses were analyzed using a Student's unpaired *t*-test or a non-parametric Mann–Whitney's U test, depending on applicability. Comparisons of gene expressions between left and right lungs were analyzed within the DH and the control groups using a Student's paired *t*-test after ensuring normality and equality of variance. Statistical significance was defined as $P < 0.05$. All statistical analyses were two-tailed and were performed using the SigmaStat software program (Jandel Scientific, San Rafael, CA).

RESULTS

Body and Lung Weights at Term

Of the 12 operated fetuses, 6 were alive at cesarean delivery (DH group, n = 6). Six unoperated littermates served as controls (control group, n = 6). Fetal body weight of DH fetuses was indistinguishable from that of controls (40.2 ± 3.7 g vs. 44.4 ± 5.8 g). Total, left and right LBWR were significantly decreased in DH fetuses ($P < 0.001$; Table 3).

Transcription of Genes Involved in Alveolarization

In DH fetuses, ELN gene expression was downregulated by 46% ($P = 0.004$) and 43% ($P = 0.009$) in left and right lungs, respectively, as compared with controls (Fig. 2). We also studied transcript levels of lysyl oxidase (LOX) and fibulin 5 (FBLN5), essential molecules for maintaining integrity and properties of elastic fibers.[16] Pulmonary mRNA content for LOX was diminished in DH fetuses to 74% ($P = 0.045$) and to 75% ($P = 0.043$) of the left and right control levels, respectively (Fig. 2). FBLN5 transcript was reduced by 29% and 18% in DH ipsilateral and contralateral lungs ($P = 0.04$ and $P = 0.048$, respectively). Because tenascin C (TNC) peaks during alveolarization,[17] its expression was evaluated. Despite decreased TNC mRNA levels in both DH lungs, the differences between groups were not significant (Fig. 2). Drebrin (DBN1), an actin-binding protein identified in cell projections of septal myofibroblasts, has been related to the elongation of the secondary septum during alveolarization.[18] Message expression for DBN1 was therefore studied, and was unchanged after DH induction (Fig. 2).

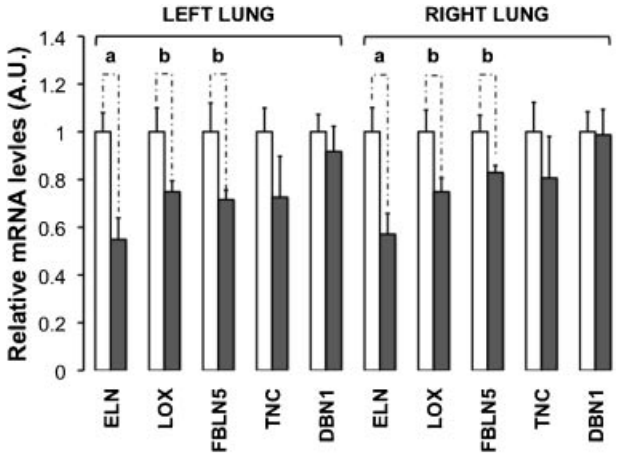

Fig. 2. Bar graph showing relative mRNA levels of alveolarization genes in left and right lungs from DH (■) and control (CTRL, □) groups. In DH fetuses compared with CTRL, ELN, LOX, and FBLN5 were downregulated bilaterally. Values are expressed as mean fold change in mRNA expression of each target gene, compared with CTRL fold, which is 1.0. Error bars represent SEM of the fold change. $^{a}P < 0.01$; $^{b}P < 0.05$. A.U. = arbitrary unit.

Transcription of NO and VEGF Signaling Genes

A drop by 29% in eNOS mRNA levels was seen in left DH lungs ($P = 0.028$; Fig. 3). There was an analogous decrease in right DH lungs, however not significant. The transition from fetus to newborn requires pulmonary vasodilatation resulting from increased activity and expression of soluble guanylate cyclases (sGC) in late gestation.[19] Meanwhile, specific phosphodiesterase 5 (PDE5), highly expressed during fetal life, decreases rapidly after birth.[20] For these reasons, we examined gene expression for PDE5, sGCα1 subunit,

TABLE 3— Lung to Body Weight Ratios in DH and Control Fetuses

Groups	Total LBWR	Left LBWR	Right LBWR
CTRL (n = 6)	0.026 ± 0.0007*	0.011 ± 0.0003*	0.016 ± 0.0006*
DH (n = 6)	0.012 ± 0.0009	0.0004 ± 0.0002	0.008 ± 0.0006

Fetal body and both lungs from DH and control (CTRL) fetuses were accurately weighed at delivery for the determination of total, left, and right lung to body weight ratios (LBWR). Values are expressed as mean ± SEM.
*$P < 0.001$.

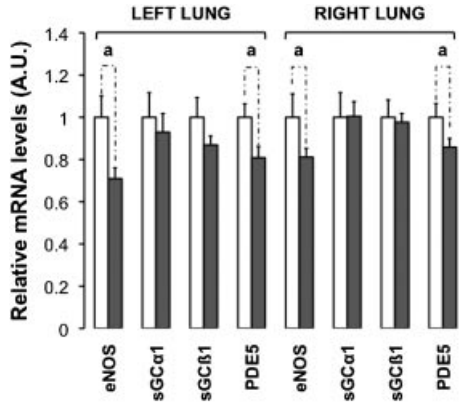

Fig. 3. Bar graph illustrating relative mRNA expression of genes involved in the NO/cGMP signaling pathway in left and right lungs from DH (■) and control (CTRL, □) groups. Down-regulation of eNOS occurred in the left lung of DH fetuses compared with the left lung of CTRL. Gene expression levels for PDE5 were reduced bilaterally. Values are expressed as mean fold change in each target gene, compared with CTRL fold, which is 1.0. Error bars illustrate SEM of the fold change. $^{a}P < 0.05$. A.U. = arbitrary unit.

and sGCß1 subunit. In DH lungs, mRNA levels for PDE5 were decreased by 19% and 16% in left and right lungs respectively, as compared with controls ($P = 0.05$ and $P = 0.04$; Fig. 3). Expressions of sGCα1 and sGCß1 were not significantly modulated. Message expression for VEGF and its receptors (VEGFR1 and VEGFR2) was unchanged after DH creation (Fig. 4).

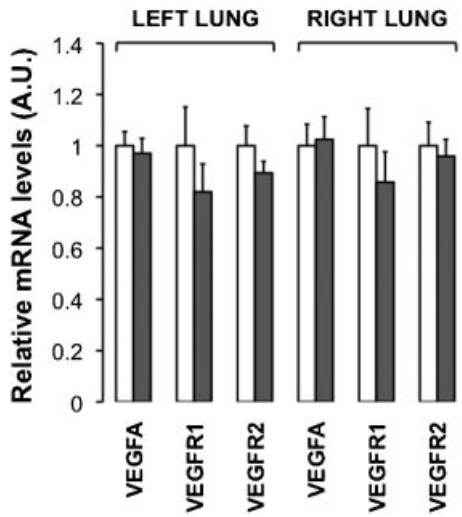

Fig. 4. Bar graph showing relative mRNA levels of genes involved in the VEGF signaling pathway in left and right lungs from DH (■) and control (CTRL, □) groups. mRNA levels for VEGFA, VEGFR1, and VEGFR2 were not changed after DH creation. Values are expressed as mean fold change in each target gene, compared with CTRL fold, which is 1.0. Error bars represent SEM of the fold change. A.U. = arbitrary unit.

Transcription of Genes Encoding Surfactant-Associated Proteins

SPC transcripts were increased by 32% in the left DH lungs ($P = 0.004$). There was no significant effect of DH creation on lung mRNA contents for SPA and SPB (Fig. 5).

DISCUSSION

In the fetal rabbit model for CDH, hypoplastic lungs exhibited a downregulation of the transcription of genes involved in alveolarization, angiogenesis, and regulation of pulmonary vascular tone, without changes in the surfactant axis. Most of these observations were consistent with those of humans, giving more confidence in the rabbit model. Moreover, this work highlighted mechanisms that could underlie CDH pathogenesis, and suggested potential targets for antenatal therapies.

qPCR is considered as the gold standard to study the transcriptome and allows the use of small amounts of starting material, which is advantageous with regard to hypoplastic tissue. Recently, microarray technology has established gene expression profile in the CDH rat model.[21] Despite useful information provided about the expression of hundreds of genes, many issues are raised by this concept. Instead of exploring the genome, we used qPCR to focus on specific target genes that may be relevant in the setting of CDH.

The rabbit is an appropriate small animal for experiments occurring in late gestation. We preferred the rabbit

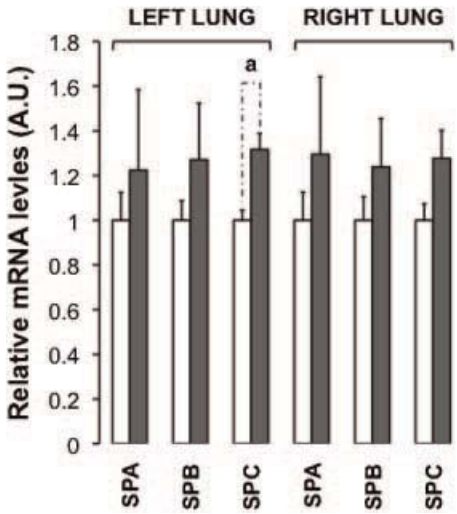

Fig. 5. Bar graph showing relative mRNA expression of surfactant associated protein genes in left and right lungs from DH (■) and control (CTRL, □) groups. In DH fetuses compared with CTRL, mRNA levels for SPC in the left lung were increased whereas SPA and SPB mRNA levels remained unchanged. Values are expressed as mean fold change in each target gene, with the CTRL group as calibrator. Error bars show SEM of the fold change. $^{a}P < 0.01$. A.U. = arbitrary unit.

model mainly because pulmonary development in this species mimics largely that of humans,[22] unlike in sheep[23] and rats.[24] DH lungs in fetal rabbits displayed features of pulmonary hypoplasia, with both airways and vascular abnormalities.[10,11] At functional levels, neonatal rabbits with DH had lower compliance and higher airway resistance, tissue damping, and tissue elastance.[12] This, together with new data of the present work, helped to further validate the CDH rabbit model.

A number of limitations to this study should be noted. First, our experimental model is not perfect as shown by discrepancies with human CDH findings, a common issue encountered by most animal models. Another weakness of our experimental design is the absence of sham-operated fetuses serving as controls. In the rabbit model, sham-operated fetuses did not differ from unoperated littermates in terms of fetal growth, LBWR, and histology.[10,11] Nevertheless, stress, inflammation, and pain due to surgery might have induced changes in gene expression. Second, we acknowledge that the sample size was probably underestimated. As qPCR analysis has never been done before in the CDH rabbit model, sample size was estimated from experiments in other CDH models. Increasing the sample size would consolidate our observations, at the price however of an additional use in animals. Third, only changes in mRNA contents were assessed, which may not correlate with protein levels or activity. Yet, since mechanical forces regulate transcription during lung development,[25] the surgical creation of DH was likely to induce changes in gene expressions by reducing the lung volume and the amplitude of fetal breathing movements. We recognize that confirmation of these transcriptional effects by biochemical or immunohistochemical analysis is necessary.

During late pulmonary development, the alveolarization process involves ELN-producing myofibroblasts located at the tips of secondary septa. In the rabbit model, not only the transcription of ELN, but also that of LOX and FBLN5, was decreased. In agreement with CDH in humans and other animal models,[3] our results suggested a dysregulation of elastogenesis at different levels, from the transcription of ELN to that of molecules involved in assembly and stability of elastic fibers. Changes to the signaling pathways responsible for the disorganized secondary septation in CDH are unclear. Recently, defective elastogenesis in human CDH fetuses and animal models was associated to reduced fibroblast growth factor 18 (FGF18).[3] As FGF18 induced myofibroblast expression of LOX and FBLN5,[26] a deficiency in FGF18 could account for the low transcription of LOX and FBLN5. Furthermore, impaired alveolarization could originate from abnormal transforming growth factor-ß (TGFß) signaling, as supported by knockout models.[27] Because data regarding the role of TGFß in CDH are conflicting and scarce,[28,29] future investigations are warranted. Finally, knockout models have evidenced the role of the platelet-derived growth factor (PDGF) in alveologenesis.[30] Nevertheless, upregulation of PDGF in the CDH rat model has been reported only in the early stages of gestation.[31] The role of PDGF in disrupted secondary septation has to be therefore confirmed in near-term human fetuses with CDH.

The molecular mechanisms that underlie defective angiogenesis in CDH and failure of the pulmonary vasculature to adapt at birth are still poorly understood. The NO/cGMP signaling plays a major role in vascular growth during septation and modulation of perinatal pulmonary vascular tone.[32] Expression of eNOS in CDH was found reduced as evidenced by our data and those obtained from human[4] and rat[33] CDH lungs. Because NO is a downstream target of VEGF-induced angiogenesis, expressions of VEGF and its receptors were investigated in human CDH fetuses[4] and newborns.[34] In disagreement with human findings, expression of the VEGF signaling was not disturbed in the CDH rabbit model, underlining the limitations of animal models.

As CDH newborns with pulmonary hypertension are often refractory to inhaled NO, reduced cGMP-mediated pulmonary vasodilatation may be due to anomalies in sGC and PDE5 expression and/or activity. In the absence of human findings, decreased sGC activity has been reported in the lungs of DH lambs,[35] but this impairment was not supported by our data. While lungs from CDH rats showed increased PDE5 activity at birth,[36] we found a downregulation of the PDE5 gene. This discordance may reflect the fact that we harvested rabbit fetuses before the first breath, enabling postnatal adaptation to occur, and hence PDE5 levels to fall.[37] Direct activators of sGC and inhibitors of PDE5 have been proposed as effective postnatal drugs to treat or prevent neonatal pulmonary hypertension.[38] Interestingly, prenatal sildenafil promoted pulmonary vessels density and NO-mediated vasodilatation in the CDH rat model.[36] Future work is needed to address the question whether modulators of the NO/cGMP signaling—administered alone or in adjunction to TO—could rescue lung vasculature in utero and restore normal vasoreactivity before birth in human fetuses with CDH.

In the past few years, many works have addressed the question of the surfactant status in CDH, leading to contradictory results.[39,40] In recent literature, pulmonary surfactant contents from human CDH fetuses were found appropriate for lung size, indicating a normal process of epithelial maturation.[2] Our findings were not fully consistent with these human observations and shared similarities with the surgically induced CDH model in lamb.[40]

Despite the limitations of the present study, analogies between fetal rabbits with surgically induced DH and

human fetuses with CDH make this model valuable for the study of this disease at late stages of lung development. With regard to the relevance of the rabbit model to CDH, we suggested that this model may help to refine the molecular understanding of TO and to develop new potential antenatal therapies.

ACKNOWLEDGMENTS

We thank Karl Storz (Tuttlingen, Germany) for having provided the fiberscopic device for rabbit intubation. A.V. is a recipient from a grant of the Belgian ''Fonds de la Recherche Scientifique'' (FNRS).

REFERENCES

1. Stege G, Fenton A, Jaffray B. Nihilism in the 1990s: the true mortality of congenital diaphragmatic hernia. Pediatrics 2003; 112:532–535.
2. Boucherat O, Benachi A, Chailley-Heu B, Franco-Montoya ML, Elie C, Martinovic J, Bourbon JR. Surfactant maturation is not delayed in human fetuses with diaphragmatic hernia. PLoS Med 2007;4:e237.
3. Boucherat O, Benachi A, Barlier-Mur AM, Franco-Montoya ML, Martinovic J, Thébaud B, Chailley-Heu B, Bourbon JR. Decreased lung fibroblast growth factor 18 and elastin in human congenital diaphragmatic hernia and animal models. Am J Respir Crit Care Med 2007;175:1066–1077.
4. Boucherat O, Franco-Montoya ML, Delacourt C, Martinovic J, Masse V, Elie C, Thébaud B, Benachi A, Bourbon JR. Defective angiogenesis in hypoplastic human fetal lungs correlates with nitric oxide synthase deficiency that occurs despite enhanced angiopoietin-2 and VEGF. Am J Physiol Lung Cell Mol Physiol 2010;298:L849–L956.
5. Khan PA, Cloutier M, Piedboeuf B. Tracheal occlusion: a review of obstructing fetal lungs to make them grow and mature. Am J Med Genet C Semin Med Genet 2007;145C:125–138.
6. Keijzer R, Liu J, Deimling J, Tibboel D, Post M. Dual-hit hypothesis explains pulmonary hypoplasia in the nitrofen model of congenital diaphragmatic hernia. Am J Pathol 2000;156: 1299–1306.
7. Roubliova XI, Verbeken EK, Wu J, Vaast P, Jani J, Deprest JA. Effect of tracheal occlusion on peripheric pulmonary vessel muscularization in a fetal rabbit model for congenital diaphragmatic hernia. Am J Obstet Gynecol 2004;191:830–836.
8. Jani JC, Flemmer AW, Bergmann F, Gallot D, Roubliova X, Muensterer OJ, Hajek K, Deprest JA. The effect of fetal tracheal occlusion on lung tissue mechanics and tissue composition. Pediatr Pulmonol 2009;44:112–121.
9. Nelson SM, Hajivassiliou CA, Haddock G, Cameron AD, Robertson L, Olver RE, Hume R. Rescue of the hypoplastic lung by prenatal cyclical strain. Am J Respir Crit Care Med 2005;171:1395–1402.
10. Wu J, Yamamoto H, Gratacos E, Ge X, Verbeken E, Sueishi K, Hashimoto S, Vanamo K, Lerut T, Deprest J. Lung development following diaphragmatic hernia in the fetal rabbit. Hum Reprod 2000;15:2483–2488.
11. Roubliova X, Verbeken E, Wu J, Yamamoto H, Lerut T, Tibboel D, Deprest J. Pulmonary vascular morphology in a fetal rabbit model for congenital diaphragmatic hernia. J Pediatr Surg 2004;39:1066–1072.
12. Flemmer AW, Jani JC, Bergmann F, Muensterer OJ, Gallot D, Hajek K, Sugawara J, Till H, Deprest JA. Lung tissue mechanics predict lung hypoplasia in a rabbit model for congenital diaphragmatic hernia. Pediatr Pulmonol 2007;42:505–512.
13. Tran HS, Puc MM, Tran JL, Del Rossi AJ, Hewitt CW. A method of endoscopic endotracheal intubation in rabbits. Lab Anim 2001;35:249–252.
14. Vandesompele J, De Preter K, Pattyn F, Poppe B, Van Roy N, De Paepe A, Speleman F. Accurate normalization of real-time quantitative RT-PCR data by geometric averaging of multiple internal control genes. Genome Biol 2002;3:34.
15. Pfaffl MW. A new mathematical model for relative quantification in real-time RT-PCR. Nucleic Acids Res 2001;29:2002–2007.
16. Mäki JM, Sormunen R, Lippo S, Kaarteenaho-Wiik R, Soininen R, Myllyharju J. Lysyl oxidase is essential for normal development and function of the respiratory system and for the integrity of elastic and collagen fibers in various tissues. Am J Pathol 2005;167:927–936.
17. Young SL, Chang LY, Erickson HP. Tenascin-C in rat lung: distribution, ontogeny and role in branching morphogenesis. Dev Biol 1994;161:615–625.
18. Yamada M, Kurihara H, Kinoshita K, Sakai T. Temporal expression of alpha-smooth muscle actin and drebrin in septal interstitial cells during alveolar maturation. J Histochem Cytochem 2005;53:735–744.
19. Bloch KD, Filippov G, Sanchez LS, Nakane M, de la Monte SM. Pulmonary soluble guanylate cyclase, a nitric oxide receptor, is increased during the perinatal period. Am J Physiol 1997; 272:L400–L406.
20. Hanson KA, Burns F, Rybalkin SD, Miller JW, Beavo J, Clarke WR. Developmental changes in lung cGMP phosphodiesterase-5 activity, protein, and message. Am J Respir Crit Care Med 1998;158:279–288.
21. Burgos CM, Uggla AR, Fagerström-Billai F, Eklöf AC, Frenckner B, Nord M. Gene expression analysis in hypoplastic lungs in the nitrofen model of congenital diaphragmatic hernia. J Pediatr Surg 2010;45:1445–1454.
22. Kikkawa Y, Motoyama EK, Gluck L. Study of the lungs of fetal and newborn rabbits. Morphologic, biochemical, and surface physical development. Am J Pathol 1968;52:177–210.
23. Alcorn DG, Adamson TM, Maloney JE, Robinson PM. A morphologic and morphometric analysis of fetal lung development in the sheep. Anat Rec 1981;201:655–667.
24. Burri PH, Dbaly J, Weibel ER. The postnatal growth of the rat lung. I. Morphometry. Anat Rec 1974;178:711–730.
25. Liu M, Tanswell AK, Post M. Mechanical force-induced signal transduction in lung cells. Am J Physiol 1999;277:L667–L683.
26. Chailley-Heu B, Boucherat O, Barlier-Mur AM, Bourbon JR. FGF-18 is upregulated in the postnatal rat lung and enhances elastogenesis in myofibroblasts. Am J Physiol Lung Cell Mol Physiol 2005;288:L43–L51.
27. Dünker N, Krieglstein K. Targeted mutations of transforming growth factor-beta genes reveal important roles in mouse development and adult homeostasis. Eur J Biochem 2000;267:6982–6988.
28. Leinwand MJ, Zhao J, Tefft JD, Anderson KD, Warburton D. Murine nitrofen-induced pulmonary hypoplasia does not involve induction of TGF-beta signaling. J Pediatr Surg 2002;37:1123–1127.
29. Quinn TM, Sylvester KG, Kitano Y, Kitano Y, Liechty KW, Jarrett BP, Adzick NS, Flake AW. TGF-beta2 is increased after fetal tracheal occlusion. J Pediatr Surg 1999;34:701–705.
30. Lindahl P, Karlsson L, Hellström M, Gebre-Medhin S, Willetts K, Heath JK, Betsholtz C. Alveogenesis failure in PDGF-A-deficient mice is coupled to lack of distal spreading of alveolar smooth muscle cell progenitors during lung development. Development 1997;124:3943–3953.

31. Dingemann J, Doi T, Ruttenstock E, Puri P. Abnormal platelet-derived growth factor signaling accounting for lung hypoplasia in experimental congenital diaphragmatic hernia. J Pediatr Surg 2010;45:1989–1994.
32. North AJ, Star RA, Brannon TS, Ujiie K, Wells LB, Lowenstein CJ, Snyder SH, Shaul PW. Nitric oxide synthase type I and type III gene expression are developmentally regulated in rat lung. Am J Physiol 1994;266:L635–L641.
33. North AJ, Moya FR, Mysore MR, Thomas VL, Wells LB, Wu LC, Shaul PW. Pulmonary endothelial nitric oxide synthase gene expression is decreased in a rat model of congenital diaphragmatic hernia. Am J Respir Cell Mol Biol 1995;13:676–682.
34. Shehata SM, Mooi WJ, Okazaki T, El-Banna I, Sharma HS, Tibboel D. Enhanced expression of vascular endothelial growth factor in lungs of newborn infants with congenital diaphragmatic hernia and pulmonary hypertension. Thorax 1999;54:427–431.
35. Thébaud B, Petit T, De Lagausie P, Dall'Ava-Santucci J, Mercier JC, Dinh-Xuan AT. Altered guanylyl-cyclase activity in vitro of pulmonary arteries from fetal lambs with congenital diaphragmatic hernia. Am J Respir Cell Mol Biol 2002;27:42–47.
36. Luong C, Rey-Perra J, Vadivel A, Gilmour G, Sauve Y, Koonen D, Walker D, Todd KG, Gressens P, Kassiri Z, et al. Antenatal sildenafil treatment attenuates pulmonary hypertension in experimental congenital diaphragmatic hernia. Circulation 2011;123:2120–2131.
37. Farrow KN, Wedgwood S, Lee KJ, Czech L, Gugino SF, Lakshminrusimha S, Schumacker PT, Steinhorn RH. Mitochondrial oxidant stress increases PDE5 activity in persistent pulmonary hypertension of the newborn. Respir Physiol Neurobiol 2010;174:272–281.
38. Deruelle P, Balasubramaniam V, Kunig AM, Seedorf GJ, Markham NE, Abman SH. BAY 41-2272, a direct activator of soluble guanylate cyclase, reduces right ventricular hypertrophy and prevents pulmonary vascular remodeling during chronic hypoxia in neonatal rat. Biol Neonate 2006;90:135–144.
39. Van Tuyl M, Blommaart PE, Keijzer R, Wert SE, Ruijter JM, Lamers WH, Tibboel D. Pulmonary surfactant protein A, B, and C mRNA and protein expression in the nitrofen-induced congenital diaphragmatic hernia rat model. Pediatr Res 2003;54:641–652.
40. Davey MG, Biard JM, Robinson L, Tsai J, Schwarz U, Danzer E, Adzick NS, Flake AW, Hedrick HL. Surfactant protein expression is increased in the ipsilateral but not contralateral lungs of fetal sheep with left-sided diaphragmatic hernia. Pediatr Pulmonol 2005;39:359–367.